JOURNAL OF VIROLOGY, Nov. 2010, p. 11929–11936 Vol. 84, No. 22
0022-538X/10/$12.00 doi:10.1128/JVI.01658-10

Andes Virus Regulation of Cellular MicroRNAs Contributes to Hantavirus-Induced Endothelial Cell Permeability▽

Timothy Pepini,[1] Elena E. Gorbunova,[2] Irina N. Gavrilovskaya,[2] Jonathan E. Mackow,[2] and Erich R. Mackow[1,2]*

Molecular and Cellular Biology Graduate Program,[1] Department of Molecular Genetics and Microbiology,[2] Stony Brook University, Stony Brook, New York 11794-5122

Received 6 August 2010/Accepted 5 September 2010

Hantaviruses infect human endothelial cells (ECs) and cause two diseases marked by vascular permeability defects, hemorrhagic fever with renal syndrome (HFRS) and hantavirus pulmonary syndrome (HPS). Vascular permeability occurs in the absence of EC lysis, suggesting that hantaviruses alter normal EC fluid barrier functions. ECs infected by pathogenic hantaviruses are hyperresponsive to vascular endothelial growth factor (VEGF), and this alters the fluid barrier function of EC adherens junctions, resulting in enhanced paracellular permeability. Vascular permeability and VEGF-directed responses are determined by EC-specific microRNAs (miRNAs), which regulate cellular mRNA transcriptional responses. miRNAs mature within cytoplasmic processing bodies (P bodies), and the hantavirus nucleocapsid (N) protein binds RNA and localizes to P bodies, suggesting that hantaviruses may modify miRNA functions within infected ECs. Here we assessed changes in EC miRNAs following infection by the HPS-causing Andes hantavirus (ANDV). We analyzed 352 human miRNAs within ANDV-infected ECs using quantitative real-time (RT)-PCR arrays. Fourteen miRNAs, including six miRNAs that are associated with regulating vascular integrity, were upregulated >4-fold following infection by ANDV. Nine miRNAs were downregulated 3- to 3,400-fold following ANDV infection; these included miR-410, involved in regulating secretion, and miR-218, which is linked to the regulation of EC migration and vascular permeability. We further analyzed changes in miR-126, an EC-specific miRNA that regulates vascular integrity by suppressing SPRED1 and PIK3R2 mRNAs. While miR-126 levels were only slightly altered, we found that SPRED1 and PIK3R2 mRNA levels were increased 10- and 7-fold, respectively, in ANDV-infected ECs but were unaltered in ECs infected by the nonpathogenic Tula hantavirus (TULV). Consistent with increased SPRED1 expression, we found that the level of phospho-cofilin was decreased within ANDV-infected ECs. Moreover, small interfering RNA (siRNA) knockdown of SPRED1 dramatically decreased the permeability of ANDV-infected ECs in response to VEGF, suggesting that increased SPRED1 contributes to EC permeability following ANDV infection. These findings suggest that interference with normal miRNA functions contributes to the enhanced paracellular permeability of ANDV-infected ECs and that hantavirus regulation of miRNA functions is an additional determinant of hantavirus pathogenesis.

Pathogenic hantaviruses are transmitted to humans from small-mammal hosts and predominantly infect endothelial cells (ECs) (58). Hantaviruses cause one of two vascular permeability-based diseases: hemorrhagic fever with renal syndrome (HFRS) and hantavirus pulmonary syndrome (HPS) (58). Both diseases are characterized by acute thrombocytopenia, edema, and the loss of vascular integrity following EC infection (5, 10, 11, 50, 57, 58, 70). However, hantaviruses are not lytic, indicating that hantaviruses alter normal EC functions which maintain vascular integrity (50, 57, 70).

Hantaviruses are enveloped viruses containing a trisegmented, negative-sense RNA genome encoding four viral proteins (58). Hantaviruses replicate in the cytoplasm and mature by budding into the lumen of the cis-Golgi complex, where their surface glycoproteins are trafficked, and exiting cells by an aberrant secretory process (58). Pathogenic hantaviruses attach to cells by binding inactive conformations of β_3 integrin receptors present on platelets and ECs (18, 19, 22, 45, 52). At late times postinfection (p.i.), hantaviruses remain cell associated through interactions with $\alpha_v\beta_3$, and bound virus directs the adherence of quiescent platelets to the EC surface (18, 19, 22). β_3 integrins on platelets and ECs play a central role in the regulation of vascular integrity (2, 4, 9, 31, 33, 53, 54). On ECs, β_3 integrins normally regulate the permeabilizing effects of vascular endothelial growth factor (VEGF) by forming a complex with VEGF receptor 2 (VEGFR2) (4, 60). In fact, β_3 integrin knockouts are hyperresponsive to the permeabilizing effects of VEGF (31, 53, 54). Consistent with this, pathogenic hantaviruses block $\alpha_v\beta_3$-directed EC migration and enhance EC permeability in response to VEGF at 3 days after infection (20, 21, 26, 52). These findings suggest that pathogenic hantaviruses alter VEGFR2-directed signaling responses at late times after EC infection, although the mechanism by which hantaviruses enhance VEGFR2 responses remains to be defined (20, 26).

VEGFR2 responses are regulated by redundant receptor responses and signaling pathways that rapidly alter the barrier function of EC adherens junctions in order to maintain vascular integrity (12, 13, 17, 43). Recently, EC-specific microRNAs (miRNAs) have also been shown to regulate VEGF-induced

* Corresponding author. Mailing address: Dept. of Molecular Genetics & Microbiology, Stony Brook University, Life Sciences Rm. 126, Stony Brook, NY 11794-5222. Phone: (631) 632-7014. Fax: (631) 632-9797. E-mail: Erich.Mackow@stonybrook.edu.

▽ Published ahead of print on 15 September 2010.

responses and serve as key determinants of vascular permeability (16, 41, 65, 67, 68). As a result, changes in miRNA regulation could contribute to enhanced EC permeability following pathogenic hantavirus infection. miRNAs are short, noncoding RNAs, ~21 nucleotides in length, which are highly conserved (3, 6, 14, 28, 39, 69) and selectively expressed in specific cells and tissues (38, 41, 67). miRNAs regulate protein expression of specific mRNAs at a posttranscriptional level, either by directing the degradation of target mRNAs or by repressing mRNA translation (51). miR-126 is an EC-specific miRNA that is responsible for maintaining vascular integrity, and knocking out miR-126 results in increased capillary permeability and edema in mice (15, 42). miR-126 functions by repressing the expression of SPRED1 (sprouty-related EVH1 domain containing protein 1) and PIK3R2 (phosphoinositide-3-kinase, regulatory subunit 2), which are tied to downstream signaling responses directed by VEGFR2 activation (15, 36, 42, 67). Similar to knocking out miR-126, overexpressing SPRED1 alone increases VEGF-induced EC permeability, and as a result miR-126 normally enhances EC barrier functions by repressing SPRED1 activity (15, 42, 67, 68).

miR-126 and SPRED1 regulate capillary integrity by determining the phosphorylation state of cofilin (15, 36). SPRED1 is a negative regulator of the LIM family kinase TESK1 (testicular protein kinase 1), and SPRED1 binding to TESK1 inhibits cofilin phosphorylation (15, 36). Unphosphorylated cofilin severs actin filaments and disrupts adherens junctions by dissociating VE-cadherin from its cytoskeletal anchor (61). In contrast, TESK1 phosphorylation of cofilin inactivates cofilin, stabilizing actin filaments and inter-EC adherens junctions (40, 64). Since adherens junctions form the primary fluid barrier of the endothelium (12, 17), the state of cofilin phosphorylation contributes to the regulation of EC permeability.

The hantavirus nucleocapsid protein reportedly binds mRNA caps and facilitates translation of viral proteins (46, 47). Interestingly, the nucleocapsid protein was also reported to localize to cytoplasmic processing bodies (P bodies) (46), where miRNAs mature and regulate mRNA expression (3, 6, 14, 28, 39, 69). The ability of the nucleocapsid protein to bind cellular RNAs and localize to miRNA containing P bodies provides a strong rationale for hantaviruses to alter miRNA regulation within infected ECs and thereby EC permeability in response to VEGF (20).

Here we report that Andes hantavirus (ANDV) infection of human ECs results in changes in the level of specific EC miRNAs. We found that 23 miRNAs were either up- or downregulated 3- to 3,400-fold following ANDV infection. Moreover, the levels of six miRNAs which regulate angiogenesis and vascular integrity were increased >4-fold following infection, while one miRNA associated with the regulation of Robo1, a receptor that counters Robo4 regulation of VEGF responses, was downregulated 129-fold. Although there was little change in the level of miR-126 following ANDV infection, we found that its mRNA targets, SPRED1 and PIK3R2, were induced 10- and 7-fold, respectively. Increased SPRED1 mRNA levels occurred concomitantly with a decrease in phosphorylated cofilin (phospho-cofilin) in ANDV-infected ECs, and this finding correlates with increased EC permeability (20). Additionally, small interfering RNA (siRNA) knockdown of SPRED1 blocked ANDV-induced EC permeability in response to VEGF, suggesting that SPRED1 is a target for regulating hantavirus-induced EC permeability. These findings suggest that ANDV infection interferes with key miRNA-regulated EC responses that are involved in maintaining vascular integrity.

MATERIALS AND METHODS

Cells and virus. Vero E6 cells (ATCC CRL-1586) were grown in Dulbecco's modified Eagle medium (DMEM) containing 10% fetal calf serum (FCS; Sigma), penicillin (100 mg/ml), streptomycin sulfate (100 mg/ml), and amphotericin B (50 μg/ml) (GIBCO). Human umbilical vein ECs (HUVECs) were purchased from Clonetics (Walkersville, MD) and grown in EC basal medium-2 (EBM-2; Clonetics) supplemented with gentamicin (50 μg/ml), amphotericin B (50 μg/ml), and 10% FCS (Sigma). Andes virus (CHI-7913; ANDV) (45) was kindly provided by B. Hjelle (University of New Mexico). ANDV and Tula virus (TULV; Tula/Moravia/MA5302V/94) (20) were cultivated as previously described (20) in a biosafety level 3 facility and determined to be mycoplasma free (Roche). Briefly, virus was adsorbed onto Vero E6 monolayers for 1 h at 37°C, and cells were maintained in DMEM containing 2% FCS. Viral titers were determined as previously described (18, 22). HUVEC monolayers in 6-well plates were mock infected or infected with ANDV or TULV as described above at a multiplicity of infection of 1. Cells were >90% infected with ANDV or TULV as determined by immunoperoxidase staining.

Immunoperoxidase staining of hantavirus-infected cells. In order to monitor hantavirus infections, rabbit polyclonal antinucleocapsid serum directed against the NY-1V nucleocapsid protein was used to detect ANDV- and TULV-infected cells as previously described (18, 22). Briefly, infected EC monolayers were fixed with 100% methanol and incubated with antinucleocapsid serum (1:5,000). Cells were washed with phosphate-buffered saline (PBS) and incubated with goat anti-rabbit–horseradish peroxidase (HRP) secondary antibody (1:5,000; Amersham Biosciences). Monolayers were washed with PBS, and the number of infected cells was quantitated following staining with 3-amino-9-ethylcarbazole (0.026%) in 0.1 M sodium acetate, pH 5.2, and 0.03% H_2O_2 for 5 to 20 min at 37°C (22).

MicroRNA and total RNA purification. Seventy-two hours p.i., cells were lysed in Trizol (Invitrogen) for microRNA array analysis and in buffer RLT (RNeasy mini kit; Qiagen) for total RNA extraction. miRNAs were purified from mock-infected and ANDV-infected HUVECs using the RT^2 qPCR-grade miRNA isolation kit according to the manufacturer's protocol (SA Biosciences). Briefly, the aqueous phase from chloroform-extracted lysates was diluted in 100% ethanol and applied to spin columns to remove large RNA. Eluates were diluted with 100% ethanol, applied to a second column, and centrifuged. Columns were washed, centrifuged, and rinsed with ethanol (70%), and small RNAs were eluted in RNase-free water.

Total cellular RNA was extracted from mock-infected, ANDV-infected, or TULV-infected HUVECs using the RNeasy mini kit (Qiagen) according to the manufacturer's protocol. Briefly, lysates were passed through a 20-gauge needle and diluted in 70% ethanol. Samples were applied to spin columns, and RNA bound to the column was successively washed and eluted with RNase-free water.

cDNA synthesis. Purified miRNA (100 ng) was reverse transcribed using the RT^2 miRNA first-strand kit according to the manufacturer's protocol (SA Biosciences). Briefly, small RNA, a proprietary mix of miRNA reverse transcription primer plus External RNA control, miRNA buffer, miRNA enzyme mix, dithiothreitol (10 mM), and RNase-free water were combined and incubated at 37°C for 2 h and 95°C for 5 min. Total RNA (1 μg) was reverse transcribed using the Transcriptor first-strand cDNA synthesis kit (Roche) using oligo(dT)$_{18}$ primer (25°C for 10 min, 55°C for 30 min, 85°C for 5 min).

miRNA array real-time PCR. miRNA-specific cDNAs were used as templates for real-time PCR using the Human Genome miRNA PCR array according to the manufacturer's protocol (SA Biosciences). cDNA and RT^2 SYBR green PCR master mix were diluted and aliquoted into each well of a PCR array consisting of four 96-well plates specific for the Applied Biosystems 7300 RT-PCR machine. Each well contains a proprietary universal primer and a primer specific for one of 352 individual human miRNAs. Real-time PCR was performed using the following thermocycling parameters: 1 cycle of 95°C for 10 min and then 95°C for 15 s, 60°C for 40 s, and 72°C for 30 s for a total of 40 cycles.

Fold changes in miRNA expression levels were calculated using the RT^2 miRNA PCR array data analysis web-based software (SA Biosciences, Frederick, MD). Briefly, the threshold cycle (C_T) of each miRNA from ANDV-infected and mock-infected samples was normalized to that of U6 RNA levels (ΔC_T). Expression levels of normalized miRNA C_T values were calculated using the $2^{-\Delta CT}$ method (41). The fold change in expression levels of each miRNA was deter-

mined by comparing the expression levels of miRNAs within ANDV- and mock-infected HUVECs. Graphs were plotted using GraphPad Prism 5 software. Microarray data were validated by analysis of individual miRNAs using RT-PCR in triplicate.

qRT-PCR of cellular mRNAs. TaqMan primers for human SPRED1, PIK3R2, and GAPDH (glyceraldehyde-3-phosphate dehydrogenase) were purchased from Applied Biosystems. Quantitative real-time PCR (qRT-PCR) was performed in duplicate using an Applied Biosystems 7300 RT-PCR machine and the following thermocycling parameters: 50°C for 2 min, 95°C for 10 min, 95°C for 15 s, and 60°C for 1 min for 40 cycles. SPRED1 and PIK3R2 mRNA levels were normalized to GAPDH mRNA levels, and the fold change in mRNA levels were compared between ANDV- or TULV-infected and mock-infected cells (25). The fold change in SPRED1 and PIK3R2 mRNA levels was determined using the $2^{-\Delta CT}$ method and plotted (mean ± standard error of the mean [SEM]) using GraphPad Prism 5 software.

siRNA transfection. SPRED1 and PIK3R2 knockdown experiments were performed using SureSilencing small interfering RNAs (siRNAs) against SPRED1, PIK3R2, or negative-control siRNA (si-NEG2) purchased from SA Biosciences. Briefly, SureFECT reagent siRNA complexes were formed for 20 min at room temperature and applied to HUVECs. For RT-PCR analysis, total RNA was purified as described above and analyzed by qRT-PCR (25).

EC permeability assay. The permeability of ECs in response to ANDV infection was determined as previously described (20). HUVECs were plated on Costar Transwell plates (3-μm pores; Corning), and confluent monolayers were infected with pathogenic ANDV at an MOI of 0.5 or were mock infected. Three days p.i., monolayer permeability was assayed by adding 0.5 mg/ml of fluorescein isothiocyanate (FITC)-dextran and VEGF (100 ng/ml) to the upper chamber, and medium was taken from the lower chamber (100 μl) at the indicated times and assayed for the presence of FITC-dextran using a BioTek FLx800 fluorimeter. The fold change in FITC-dextran fluorescence intensity over that of mock-infected controls was used as a measure of the paracellular permeability of EC monolayers. Hantavirus infections were monitored by immunoperoxidase staining as described above (18, 22).

Western blot analysis. Western blot analysis was performed as previously described (23, 24). Briefly, HUVECs were infected with ANDV or TULV and treated with VEGF at 3 days p.i. as described above. Cells were lysed at various times after VEGF addition using 0.1% sodium dodecyl sulfate (SDS)–0.1% NP-40 lysis buffer (150 mM NaCl, 40 mM Tris-Cl, 2 mM EDTA, 10% glycerol, 5 nM sodium fluoride, 1 mM sodium pyrophosphate, 1 mM sodium orthovanadate) containing 1× protease inhibitor cocktail (Sigma). Total protein levels were determined by a bicinchoninic acid assay (Pierce), and 20 μg of protein was resolved by SDS-polyacrylamide (15%) gel electrophoresis. Proteins were transferred to nitrocellulose, blocked in 5% bovine serum albumin, and Western blotted for cofilin using polyclonal anti-cofilin antibody (3312; Cell Signaling) followed by anti-rabbit HRP-conjugated antibody (1:2,000; Amersham). To assess the level of phospho-cofilin, cofilin Western blots were stripped (2% sodium dodecyl sulfate, 62.5 mM Tris-Cl, 100 mM beta-mercaptoethanol) and reprobed using polyclonal anti-phospho-cofilin antibody (3311; Cell Signaling). Western blots were developed using enhanced chemiluminescence reagent (Amersham) and exposed to HyBlot CL autoradiography film (Denville Scientific). Results are representative of two separate experiments. Densitometric analysis was performed using ImageJ (NIH) software, and cofilin and phospho-cofilin data were plotted as means ± SEM using GraphPad Prism 5 software.

RESULTS

The ability of the hantavirus nucleocapsid protein to bind cellular mRNA and localize to cytoplasmic P bodies (46) suggests that pathogenic hantaviruses may alter the function of cellular miRNAs and the ability of miRNAs to regulate cognate mRNA targets. Here we determined whether ANDV infection of ECs alters the synthesis of cellular miRNAs. Human ECs were infected with ANDV, and 3 days p.i., small cellular RNAs were purified. The level of specific EC miRNAs was analyzed using a qRT-PCR microarray and compared to that of mock-infected controls. Analysis of 352 human miRNAs revealed that ANDV upregulated the expression of 14 miRNAs >4-fold (Fig. 1A). The levels of three miRNAs, miR-let-7d, miR-423-3p, and miR-146b-5p, increased >10-fold in

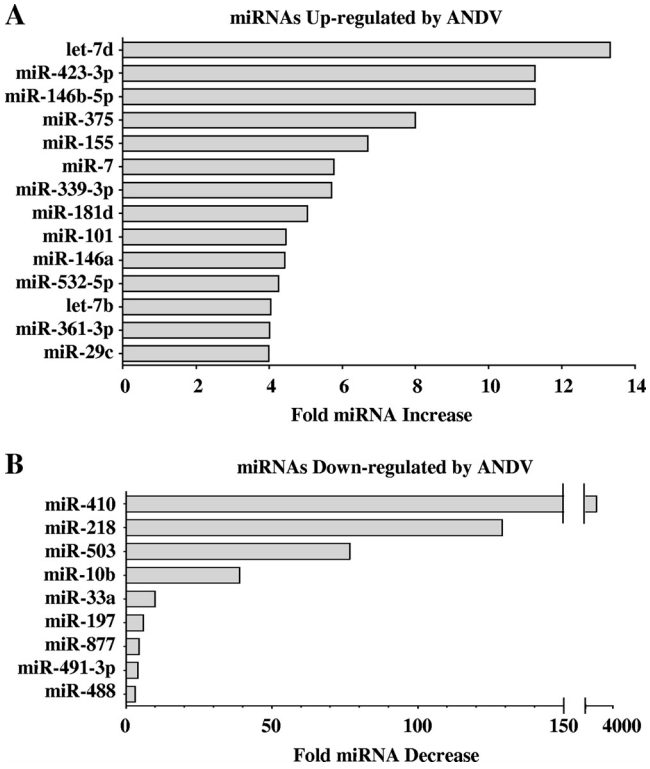

FIG. 1. miRNA qRT-PCR microarray analysis. EC monolayers were mock infected or infected with ANDV at an MOI of 1, and 3 days p.i., cells were lysed and small RNAs were purified (20). The level of 352 individual miRNAs was assessed by qRT-PCR (SA Biosciences) on an Applied Biosystems 7300 RT-PCR machine (41). miRNA levels from mock- and ANDV-infected cells were standardized to U6 RNA levels present in samples. The increase (A) or decrease (B) in miRNAs present in ANDV- versus mock-infected ECs was determined, and ≥4-fold changes in miRNA expression levels are presented.

ANDV- versus mock-infected ECs. In contrast, ANDV infection resulted in the downregulation of nine miRNAs (≥3-fold) (Fig. 1B), including miR-410, miR-218, and miR-503, which were reduced approximately 3,400-, 129-, and 77-fold, respectively. These findings demonstrate that ANDV infection of ECs results in a dramatic change in the level of specific EC miRNAs and fundamentally alters the constellation of miRNAs present within the primary cellular target of the virus.

Several miRNAs are reported to be highly expressed in ECs (41). Figure 2 confirms the high-level expression of 16 miRNAs within mock-infected ECs and evaluates changes in these miRNAs resulting from ANDV infection. The level of the most highly expressed EC miRNA, miR-503, was decreased approximately 77-fold following ANDV infection (Fig. 2). Despite this, miR-503 remains the most abundant miRNA present within ANDV-infected ECs. The level of miR-126, which has a known function in regulating vascular permeability, increased approximately 2-fold following ANDV infection (Fig. 2). In contrast, we observed a striking 3,400-fold reduction in the level of miR-410 following ANDV infection. Although miR-410-specific mRNA targets have yet to be defined, miR-410 expression was recently associated with enhancing cellular secretion (29). These findings indicate that ANDV substantially alters the level of EC-specific miRNAs and fur-

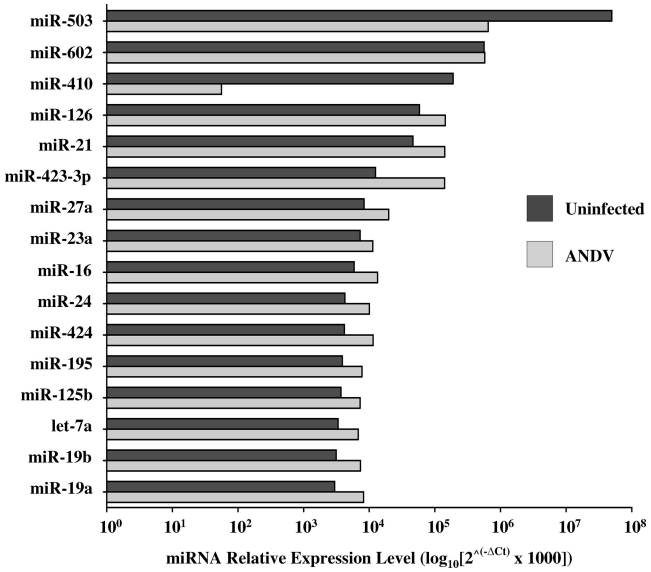

FIG. 2. Relative miRNA levels following ANDV infection. miRNAs present in ANDV- and mock-infected controls were determined by qRT-PCR of cellular miRNAs as described in the legend to Fig. 1 and standardized to U6 RNA levels. The relative levels of highly expressed EC miRNAs were determined using the $2^{-\Delta CT}$ method and are comparatively presented (41).

ther suggests that changes in miRNA regulation may contribute to altered EC functions following infection.

miRNAs have been reported to play critical roles in the regulation of angiogenesis and EC permeability (67, 68). Analysis of the microarray data revealed that six miRNAs involved in angiogenesis (miR-155, -320, -27b, -222, -21, and -378) were upregulated approximately 3- to 7-fold following ANDV infection (Fig. 3). While the mechanism by which a number of these miRNAs regulate angiogenesis and EC functions has not been determined, miR-155, miR-320, and miR-222 have been shown to have important roles in the regulation of EC responses to growth factors, including VEGF, or are linked to the maintenance of capillary integrity (16, 49, 68). These findings indicate that ANDV infection alters miRNAs which regulate EC integrity, and this further suggests the importance of analyzing EC

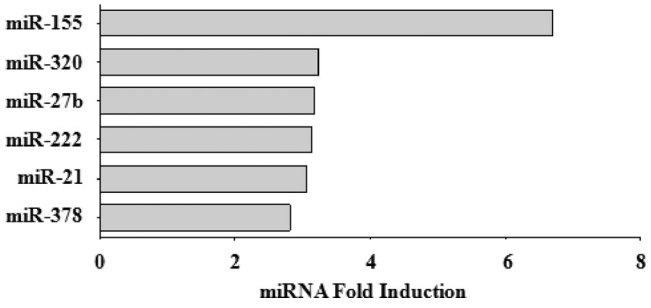

FIG. 3. Angiogenic miRNAs induced by ANDV infection. The relative levels of cellular miRNAs present within mock- and ANDV-infected ECs were determined as described in the legend to Fig. 1. Changes in miRNAs reported to play a role in angiogenesis (49, 68) are presented as the fold increase in miRNAs present in ANDV-infected ECs relative to that in mock-infected ECs.

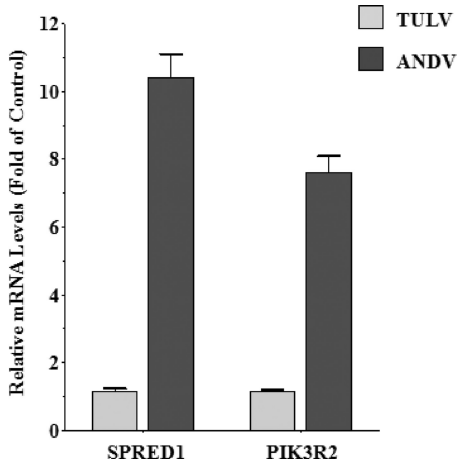

FIG. 4. SPRED1 and PIK3R2 mRNA induction following ANDV infection. HUVECs were infected with ANDV or TULV (MOI of 1) or were mock infected. Three days p.i., SPRED1 and PIK3R2 mRNA levels were determined by quantitative real-time PCR. SPRED1 and PIK3R2 mRNA levels were standardized to constant GAPDH mRNA levels. Data are presented as the fold change in mRNA levels relative to those of mock-infected controls using the $2^{-\Delta CT}$ method (41).

miRNAs and miRNA targets in understanding hantavirus regulation of the endothelium.

SPRED1 and PIK3R2 mRNA levels are increased following ANDV infection. miR-126 is an EC-specific miRNA that normally inhibits VEGF-directed vascular permeability. miR-126 functions by downregulating mRNAs encoding SPRED1 and PIK3R2, effectively blocking SPRED1 and PIK3R2 functions (15). Although we observed a 2-fold increase in miR-126 levels following ANDV infection (Fig. 2), it was unclear whether this change resulted in altered levels of cellular mRNAs. In order to determine if hantaviruses impede miR-126 function, we analyzed at 3 days p.i. the level of SPRED1 and PIK3R2 mRNAs within ECs infected by pathogenic ANDV and nonpathogenic TULV. Using qRT-PCR, we found that SPRED1 and PIK3R2 mRNA levels were induced 10- and 7-fold, respectively, following ANDV infection (Fig. 4). In contrast, no changes in the levels of SPRED1 or PIK3R2 mRNAs were observed following infection with TULV (Fig. 4). These data indicate that ANDV infection increased SPRED1 and PIK3R2 mRNA levels without decreasing miR-126. As a result, ANDV interferes with the normal function of miR-126 in regulating its cognate mRNA, and this finding demonstrates that ANDV induces cellular transcriptional responses associated with enhancing EC permeability.

ANDV infection decreases phosphorylation of cofilin. SPRED1 binding to TESK1 inhibits cofilin phosphorylation and enhances the dissociation of adherens junctions and EC permeability (36). In order to determine if increased SPRED1 mRNA levels were functionally significant (Fig. 4), we determined whether there was an effect on cofilin phosphorylation following pathogenic ANDV or nonpathogenic TULV infection of ECs. The level of phospho-cofilin was substantially lower in ANDV-infected ECs than TULV-infected ECs at all time points after VEGF addition (Fig. 5A) and quantitatively resulted in a 30 to 50% decrease in phospho-cofilin levels in ANDV-infected cells (Fig. 5B). These findings are consistent

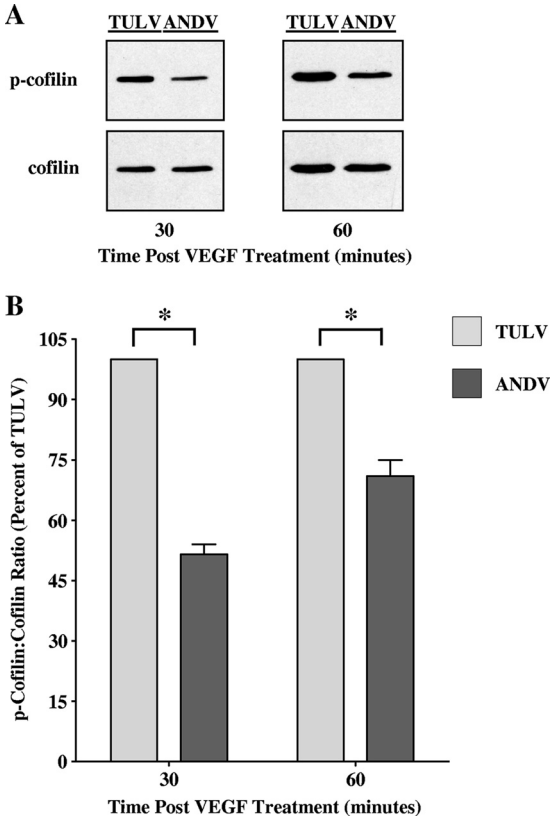

FIG. 5. Decreased cofilin phosphorylation in ANDV-infected ECs following VEGF treatment. (A) Cofilin phosphorylation within ANDV-infected ECs following VEGF treatment was assessed by Western blotting. HUVECs were infected with ANDV or TULV (MOI of 0.5), and at 3 days p.i., cells were treated with VEGF for the indicated times. Equivalent amounts of total protein were separated by SDS-polyacrylamide (15%) gel electrophoresis and analyzed by Western blotting using anti-cofilin or anti-phospho-cofilin rabbit polyclonal antibodies (Cell Signaling), HRP-conjugated anti-rabbit secondary antibody (Amersham), and enhanced chemiluminescence (Amersham). Ninety percent of cells were infected by ANDV and TULV, respectively. (B) Densitometric analysis of cofilin and phospho-cofilin levels was performed using ImageJ (NIH) software, and data were plotted as the means ± SEM using GraphPad Prism 5 software. *, $P < 0.005$.

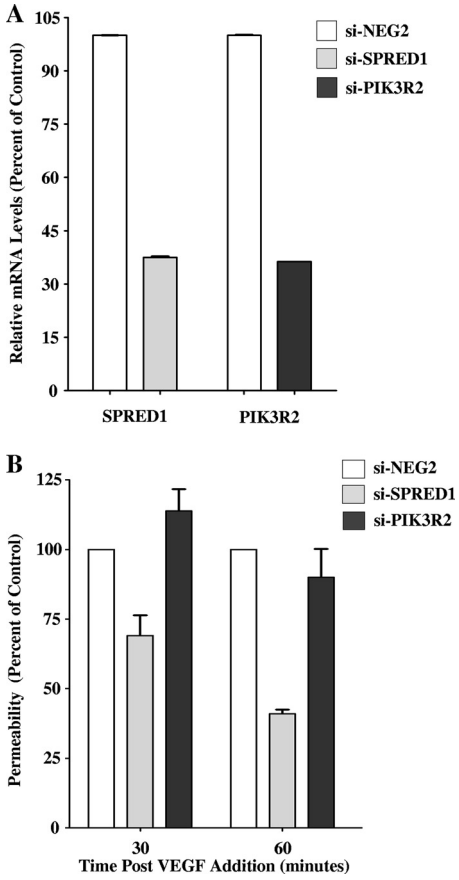

FIG. 6. SPRED1 knockdown inhibits ANDV-induced EC permeability. (A) ECs were transfected with SPRED1, PIK3R2, or a scrambled siRNA, and the levels of SPRED1 and PIK3R2 mRNAs were analyzed by qRT-PCR. mRNA levels were quantitated and standardized as described in the legend to Fig. 4 and are presented as a percentage of the levels of controls. (B) EC permeability was determined as previously described (20). One day after transfection with SPRED1, PIK3R2, or scrambled siRNAs, ECs were infected with ANDV or were mock infected. Three days p.i., FITC-dextran and VEGF were added to media in the upper chamber, and the presence of FITC-dextran in the lower chamber was quantitated after 30 or 60 min as a measure of EC permeability (20). Results are expressed as the percent monolayer permeability relative to the basal permeability levels of controls.

with an increase in SPRED1 function within ANDV-infected cells and suggest that SPRED1 induction may contribute to the enhanced permeability of ANDV-infected ECs in response to VEGF.

Knockdown of endogenous SPRED1 decreased ANDV-induced EC permeability. SPRED1 overexpression results in increased vascular permeability (15), and from our findings, both SPRED1 levels and SPRED1 functions are increased in ANDV-infected ECs. In order to determine if SPRED1 induction contributes to the enhanced permeability of hantavirus-infected cells, we transfected ECs with SPRED1 siRNAs and assayed ANDV-induced EC permeability. ECs transfected with SPRED1 or PIK3R2 siRNAs specifically reduced SPRED1 or PIK3R2 mRNAs, respectively, by 60 to 65% (Fig. 6A). Interestingly, siRNA knockdown of SPRED1 inhibited ANDV-induced permeability in response to VEGF by 30 to 60% compared to that of ECs transfected with a control siRNA or siRNA to PIK3R2 (Fig. 6B). These findings demonstrate that the induction of SPRED1 within ANDV-infected cells contributes to the enhanced permeability of ANDV-infected ECs and further suggests a specific target for regulating ANDV-induced permeability.

DISCUSSION

miRNAs are emerging as prominent regulatory molecules that play important roles in cancer, angiogenesis, and cell type specificity (7, 27, 30, 32, 38, 48, 49, 56, 65). Discrete miRNAs are required for viral infection of specific cell types and thereby contribute to the cell and tissue tropism of viruses and their sequelae (15, 16, 55, 56, 67, 68). ECs contain a unique constellation of miRNAs that contribute to the cell type-specific expression of cellular proteins within the endothelium and regulate EC functions which control vascular permeability (41).

Several EC miRNAs are associated with regulating angiogenesis, growth factor-activated pathways, or cell-cell interactions that control EC fluid barrier functions (15, 16, 55, 67, 68).

Tissue edema is a hallmark of pathogenic hantavirus infections regardless of whether infection results in hemorrhagic disease (HFRS) or acute pulmonary edema (HPS) (5, 10, 11, 50, 57, 58, 70). Pathogenic hantaviruses infect the EC lining of capillaries and enhance the permeability of ECs in response to VEGF at late times p.i. (20). Hantaviruses traffic the RNA binding nucleocapsid protein to cellular P bodies (46), where miRNAs mature (3, 6, 14), suggesting that hantaviruses might alter EC functions by interfering with normal miRNA regulatory functions. In this study, we examined the effects of ANDV on miRNA expression within infected ECs. Our results indicate that ANDV infection alters the expression of a number of EC miRNAs, including a subset which plays an important role in EC migration, adherence, and angiogenesis.

ANDV infection increased the level of six miRNAs which have recently been shown to play roles in regulating angiogenesis or vascular integrity, including miR-155, miR-320, and miR-222 (Fig. 3) (15, 16, 55, 67, 68). These miRNAs reportedly regulate adherens junction disassembly, cell migration, and cell morphology, which contribute to changes in vascular permeability (16, 49, 68). However, the role of these miRNAs in hantavirus infection of ECs remains to be defined.

ANDV infection of ECs resulted in a dramatic 3,400-fold downregulation of miR-410 (Fig. 1B). The function of miR-410 is just beginning to be disclosed, and this miRNA has not been studied in ECs. However, knockdown of miR-410 decreases cellular secretion, while increased miR-410 appears to increase secretory responses (29). At this point it is unclear whether secretion is impaired in ANDV-infected ECs or whether decreased or aberrant secretion might play a role in regulating cellular activation or immune recognition of ANDV-infected ECs. However, the dramatic reduction in miR-410 suggests that downregulating this prominently expressed endothelial miRNA may play an important role in the success of hantaviruses within their unique EC niche. This provocative finding may prove interesting as specific miR-410 targets are defined and the role of miR-410 in regulating EC functions is disclosed.

Microarray analysis further revealed a 129-fold decrease in miR-218 in ANDV-infected ECs (Fig. 1B). A recent paper has determined that miR-218 specifically downregulates the expression of Robo1, a cell surface receptor that enhances angiogenesis by inhibiting the normal VEGF regulatory responses of another EC receptor, Robo4 (1, 59, 63). Robo4 normally stabilizes the vasculature by counteracting VEGF signaling responses that result in EC hyperpermeability (1, 37). In contrast, increased Robo1 expression results in the formation of heterodimeric Robo1-Robo4 complexes which decrease cell-cell adherence and enhance EC migration (8, 34, 59, 66). This finding suggests that in ANDV-infected ECs, decreased miR-218 levels may enhance VEGF-directed permeability by increasing Robo1 and thereby decreasing Robo4 regulation. However, roles for miR-218, Robo1, and Robo4, in the enhanced VEGF-directed permeability of ANDV-infected ECs, require further investigation.

Similarly, miR-126 is an EC-specific miRNA which regulates VEGF-induced vascular permeability by repressing the expression of SPRED1 (15, 16, 67). SPRED1 induces actin turnover and is tied to the increased paracellular permeability of ECs. SPRED1 functions by binding TESK1 and blocking TESK1 phosphorylation of cofilin (15, 36). Unphosphorylated cofilin increases the disassembly of actin filaments, resulting in the internalization of VE-cadherin and the disassembly of adherens junctions that maintain a paracellular fluid barrier (62, 67, 68). In fact, overexpressing SPRED1 or knocking out miR-126 results in EC permeability in response to VEGF (15, 36, 67). Curiously, we observed only a small increase in miR-126 (2-fold) within ANDV-infected ECs, but this did not result in a decrease in SPRED1 mRNA levels. In fact, counter to increased miR-126 levels, we observed a 10-fold increase in SPRED1 mRNA following ANDV infection (Fig. 4), which is consistent with the enhanced permeability of ANDV-infected ECs (Fig. 2).

Decreased cofilin phosphorylation within ANDV-infected ECs compared to TULV-infected ECs (Fig. 5) was also consistent with observed increases in SPRED1 and suggested that ANDV interfered with normal miR-126 regulation of SPRED1 following infection. In fact, the response to SPRED1 overexpression is similar to the enhanced permeability of ECs infected by pathogenic hantaviruses (15, 20). When we analyzed the effect of SPRED1 downregulation on the permeability of ANDV-infected cells, we found that SPRED1 siRNAs both reduced SPRED1 mRNA levels (Fig. 6A) and inhibited EC permeability following ANDV infection (Fig. 6B). Increased SPRED1 levels in ANDV-infected ECs may increase cofilin activity and enhance adherens junction disassembly responses (15, 16, 26, 36). These data demonstrate that increased SPRED1 contributes to the permeability of ANDV-infected ECs. As a result, our findings link alterations in cellular VEGF responses to a potential mechanism for the enhanced paracellular permeability of hantavirus-infected ECs.

A new paper also ties miR-503 to altered regulation of cofilin responses, and thereby decreased adherence junction stability, within ANDV-infected ECs (35, 44). ANDV infection resulted in a 77-fold decrease in miR-503 within ECs (Fig. 1B and 2), and miR-503 regulates the expression of cyclin D1 (35). While cyclin D1 knockouts display increased cellular adherence, increased cyclin D1 expression decreases cellular adherence and enhances cell migration by inhibiting Rho/ROCK signaling responses (44). LIM kinase, which phosphorylates cofilin, is a key ROCK substrate, and, thus, a reduction in miR-503 levels could also contribute to the enhanced cofilin activity and enhanced EC permeability observed in ANDV-infected ECs (44). These findings suggest that additional miRNAs may contribute to hantavirus-induced EC permeability and provide additional targets for therapeutic consideration (44).

Our results indicate that ANDV interferes with both miRNA expression and the ability of miRNAs to regulate their cognate target mRNAs within ECs. The ability of the hantavirus nucleocapsid protein to bind RNA and localize to cytoplasmic P bodies (46) provides a potential means for the nucleocapsid protein to interfere with the function of miR-126, and other miRNAs, within ANDV-infected ECs. However, the ability of the hantavirus nucleocapsid protein or other viral proteins to regulate miRNA functions remains to be explored.

Collectively, these studies suggest the potential for blocking

hantavirus-induced EC permeability at several cellular points. miRNAs and mRNAs may be targeted for regulation and contribute to reducing EC permeability in response to ANDV infection (20). In addition, SPRED1, TESK1, and VE-cadherin responses (26), as well as other pathway specific targets that regulate VEGF-induced signaling responses (20), may also be considered potential therapeutic targets for reducing hantavirus-induced permeability and restoring EC barrier functions.

ACKNOWLEDGMENTS

We thank Valery Matthys for helpful discussions and critical review of the manuscript. We thank Brian Hjelle at the University of New Mexico for providing Andes virus for these studies.

This work was supported by National Institutes of Health grants R01AI47873, PO1AI055621, R21AI1080984, and U54AI57158 (Northeast Biodefense Center [director, W. I. Lipkin]).

REFERENCES

1. **Acevedo, L. M., S. M. Weis, and D. A. Cheresh.** 2008. Robo4 counteracts VEGF signaling. Nat. Med. **14:**372–373.
2. **Baker, E. K., E. C. Tozer, M. Pfaff, S. J. Shattil, J. C. Loftus, and M. H. Ginsberg.** 1997. A genetic analysis of integrin function: Glanzmann thrombasthenia in vitro. Proc. Natl. Acad. Sci. U. S. A. **94:**1973–1978.
3. **Bartel, D. P.** 2004. MicroRNAs: genomics, biogenesis, mechanism, and function. Cell **116:**281–297.
4. **Borges, E., Y. Jan, and E. Ruoslahti.** 2000. Platelet-derived growth factor receptor beta and vascular endothelial growth factor receptor 2 bind to the beta 3 integrin through its extracellular domain. J. Biol. Chem. **275:**39867–39873.
5. **Chen, J. P., and T. M. Cosgriff.** 2000. Hemorrhagic fever virus-induced changes in hemostasis and vascular biology. Blood Coagul. Fibrinolysis **11:**461–483.
6. **Chen, K., and N. Rajewsky.** 2007. The evolution of gene regulation by transcription factors and microRNAs. Nat. Rev. Genet. **8:**93–103.
7. **Choy, E. Y., K. L. Siu, K. H. Kok, R. W. Lung, C. M. Tsang, K. F. To, D. L. Kwong, S. W. Tsao, and D. Y. Jin.** 2008. An Epstein-Barr virus-encoded microRNA targets PUMA to promote host cell survival. J. Exp. Med. **205:**2551–2560.
8. **Cirulli, V., and M. Yebra.** 2007. Netrins: beyond the brain. Nat. Rev. Mol. Cell Biol. **8:**296–306.
9. **Coller, B. S.** 1997. GPIIb/IIIa antagonists: pathophysiologic and therapeutic insights from studies of c7E3 Fab. Thromb. Haemost. **78:**730–735.
10. **Cosgriff, T. M., H. W. Lee, A. F. See, D. B. Parrish, J. S. Moon, D. J. Kim, and R. M. Lewis.** 1991. Platelet dysfunction contributes to the haemostatic defect in haemorrhagic fever with renal syndrome. Trans. R. Soc. Trop. Med. Hyg. **85:**660–663.
11. **Cosgriff, T. M., and R. M. Lewis.** 1991. Mechanisms of disease in hemorrhagic fever with renal syndrome. Kidney Int. Suppl. **35:**S72–S79.
12. **Dejana, E., F. Orsenigo, and M. G. Lampugnani.** 2008. The role of adherens junctions and VE-cadherin in the control of vascular permeability. J. Cell Sci. **121:**2115–2122.
13. **Dvorak, H. F.** 2006. Discovery of vascular permeability factor (VPF). Exp. Cell Res. **312:**522–526.
14. **Eulalio, A., I. Behm-Ansmant, D. Schweizer, and E. Izaurralde.** 2007. P-body formation is a consequence, not the cause, of RNA-mediated gene silencing. Mol. Cell. Biol. **27:**3970–3981.
15. **Fish, J. E., M. M. Santoro, S. U. Morton, S. Yu, R. F. Yeh, J. D. Wythe, K. N. Ivey, B. G. Bruneau, D. Y. Stainier, and D. Srivastava.** 2008. miR-126 regulates angiogenic signaling and vascular integrity. Dev. Cell **15:**272–284.
16. **Fish, J. E., and D. Srivastava.** 2009. MicroRNAs: opening a new vein in angiogenesis research. Sci. Signal. **2:**pe1.
17. **Gavard, J., and J. S. Gutkind.** 2006. VEGF controls endothelial-cell permeability by promoting the beta-arrestin-dependent endocytosis of VE-cadherin. Nat. Cell Biol. **8:**1223–1234.
18. **Gavrilovskaya, I. N., E. J. Brown, M. H. Ginsberg, and E. R. Mackow.** 1999. Cellular entry of hantaviruses which cause hemorrhagic fever with renal syndrome is mediated by β3 integrins. J. Virol. **73:**3951–3959.
19. **Gavrilovskaya, I. N., E. E. Gorbunova, and E. R. Mackow.** 2010. Pathogenic hantaviruses direct the adherence of quiescent platelets to infected endothelial cells. J. Virol. **84:**4832–4839.
20. **Gavrilovskaya, I. N., E. E. Gorbunova, N. A. Mackow, and E. R. Mackow.** 2008. Hantaviruses direct endothelial cell permeability by sensitizing cells to the vascular permeability factor VEGF, while angiopoietin 1 and sphingosine 1-phosphate inhibit hantavirus-directed permeability. J. Virol. **82:**5797–5806.
21. **Gavrilovskaya, I. N., T. Peresleni, E. Geimonen, and E. R. Mackow.** 2002. Pathogenic hantaviruses selectively inhibit β3 integrin directed endothelial cell migration. Arch. Virol. **147:**1913–1931.
22. **Gavrilovskaya, I. N., M. Shepley, R. Shaw, M. H. Ginsberg, and E. R. Mackow.** 1998. β3 integrins mediate the cellular entry of hantaviruses that cause respiratory failure. Proc. Natl. Acad. Sci. U. S. A. **95:**7074–7079.
23. **Geimonen, E., I. Fernandez, I. N. Gavrilovskaya, and E. R. Mackow.** 2003. Tyrosine residues direct the ubiquitination and degradation of the NY-1 hantavirus G1 cytoplasmic tail. J. Virol. **77:**10760–10868.
24. **Geimonen, E., R. LaMonica, K. Springer, Y. Farooqui, I. N. Gavrilovskaya, and E. R. Mackow.** 2003. Hantavirus pulmonary syndrome-associated hantaviruses contain conserved and functional ITAM signaling elements. J. Virol. **77:**1638–1643.
25. **Geimonen, E., S. Neff, T. Raymond, S. S. Kocer, I. N. Gavrilovskaya, and E. R. Mackow.** 2002. Pathogenic and nonpathogenic hantaviruses differentially regulate endothelial cell responses. Proc. Natl. Acad. Sci. U. S. A. **99:**13837–13842.
26. **Gorbunova, E., I. N. Gavrilovskaya, and E. R. Mackow.** 2010. Pathogenic hantaviruses Andes virus and Hantaan virus induce adherens junction disassembly by directing vascular endothelial cadherin internalization in human endothelial cells. J. Virol. **84:**7405–7411.
27. **Grassmann, R., and K. T. Jeang.** 2008. The roles of microRNAs in mammalian virus infection. Biochim. Biophys. Acta **1779:**706–711.
28. **He, L., and G. J. Hannon.** 2004. MicroRNAs: small RNAs with a big role in gene regulation. Nat. Rev. Genet. **5:**522–531.
29. **Hennessy, E., M. Clynes, P. B. Jeppesen, and L. O'Driscoll.** 2010. Identification of microRNAs with a role in glucose stimulated insulin secretion by expression profiling of MIN6 cells. Biochem. Biophys. Res. Commun. **396:**457–462.
30. **Heusschen, R., M. van Gink, A. W. Griffioen, and V. L. Thijssen.** 2010. MicroRNAs in the tumor endothelium: novel controls on the angioregulatory switchboard. Biochim. Biophys. Acta **1805:**87–96.
31. **Hodivala-Dilke, K. M., K. P. McHugh, D. A. Tsakiris, H. Rayburn, D. Crowley, M. Ullman-Cullere, F. P. Ross, B. S. Coller, S. Teitelbaum, and R. O. Hynes.** 1999. Beta3-integrin-deficient mice are a model for Glanzmann thrombasthenia showing placental defects and reduced survival. J. Clin. Invest. **103:**229–238.
32. **Hussain, M., R. J. Taft, and S. Asgari.** 2008. An insect virus-encoded microRNA regulates viral replication. J. Virol. **82:**9164–9170.
33. **Hynes, R. O.** 2002. Integrins: bidirectional, allosteric signaling machines. Cell **110:**673–687.
34. **Jain, R. K., E. di Tomaso, D. G. Duda, J. S. Loeffler, A. G. Sorensen, and T. T. Batchelor.** 2007. Angiogenesis in brain tumours. Nat. Rev. Neurosci. **8:**610–622.
35. **Jiang, Q., M. G. Feng, and Y. Y. Mo.** 2009. Systematic validation of predicted microRNAs for cyclin D1. BMC Cancer **9:**194.
36. **Johne, C., D. Matenia, X. Y. Li, T. Timm, K. Balusamy, and E. M. Mandelkow.** 2008. Spred1 and TESK1—two new interaction partners of the kinase MARKK/TAO1 that link the microtubule and actin cytoskeleton. Mol. Biol. Cell **19:**1391–1403.
37. **Jones, C. A., N. R. London, H. Chen, K. W. Park, D. Sauvaget, R. A. Stockton, J. D. Wythe, W. Suh, F. Larrieu-Lahargue, Y. S. Mukouyama, P. Lindblom, P. Seth, A. Frias, N. Nishiya, M. H. Ginsberg, H. Gerhardt, K. Zhang, and D. Y. Li.** 2008. Robo4 stabilizes the vascular network by inhibiting pathologic angiogenesis and endothelial hyperpermeability. Nat. Med. **14:**448–453.
38. **Jopling, C. L., K. L. Norman, and P. Sarnow.** 2006. Positive and negative modulation of viral and cellular mRNAs by liver-specific microRNA miR-122. Cold Spring Harbor Symp. Quant. Biol. **71:**369–376.
39. **Kim, V. N., J. Han, and M. C. Siomi.** 2009. Biogenesis of small RNAs in animals. Nat. Rev. Mol. Cell Biol. **10:**126–139.
40. **Kobayashi, M., M. Nishita, T. Mishima, K. Ohashi, and K. Mizuno.** 2006. MAPKAPK-2-mediated LIM-kinase activation is critical for VEGF-induced actin remodeling and cell migration. EMBO J. **25:**713–726.
41. **Kuehbacher, A., C. Urbich, A. M. Zeiher, and S. Dimmeler.** 2007. Role of Dicer and Drosha for endothelial microRNA expression and angiogenesis. Circ. Res. **101:**59–68.
42. **Kuhnert, F., M. R. Mancuso, J. Hampton, K. Stankunas, T. Asano, C. Z. Chen, and C. J. Kuo.** 2008. Attribution of vascular phenotypes of the murine Egfl7 locus to the microRNA miR-126. Development **135:**3989–3993.
43. **Lampugnani, M. G., F. Orsenigo, M. C. Gagliani, C. Tacchetti, and E. Dejana.** 2006. Vascular endothelial cadherin controls VEGFR-2 internalization and signaling from intracellular compartments. J. Cell Biol. **174:**593–604.
44. **Li, Z., C. Wang, G. C. Prendergast, and R. G. Pestell.** 2006. Cyclin D1 functions in cell migration. Cell Cycle **5:**2440–2442.
45. **Matthys, V. S., E. E. Gorbunova, I. N. Gavrilovskaya, and E. R. Mackow.** 2010. Andes virus recognition of human and Syrian hamster β3 integrins is determined by an L33P substitution in the PSI domain. J. Virol. **84:**352–360.
46. **Mir, M. A., W. A. Duran, B. L. Hjelle, C. Ye, and A. T. Panganiban.** 2008. Storage of cellular 5′ mRNA caps in P bodies for viral cap-snatching. Proc. Natl. Acad. Sci. U. S. A. **105:**19294–19299.

47. **Mir, M. A., and A. T. Panganiban.** 2008. A protein that replaces the entire cellular eIF4F complex. EMBO J. **27:**3129–3139.
48. **Nair, V., and M. Zavolan.** 2006. Virus-encoded microRNAs: novel regulators of gene expression. Trends Microbiol. **14:**169–175.
49. **Nicoloso, M. S., R. Spizzo, M. Shimizu, S. Rossi, and G. A. Calin.** 2009. MicroRNAs—the micro steering wheel of tumour metastases. Nat. Rev. Cancer **9:**293–302.
50. **Nolte, K. B., R. M. Feddersen, K. Foucar, S. R. Zaki, F. T. Koster, D. Madar, T. L. Merlin, P. J. McFeeley, E. T. Umland, and R. E. Zumwalt.** 1995. Hantavirus pulmonary syndrome in the United States: a pathological description of a disease caused by a new agent. Hum. Pathol. **26:**110–120.
51. **Pauley, K. M., T. Eystathioy, A. Jakymiw, J. C. Hamel, M. J. Fritzler, and E. K. Chan.** 2006. Formation of GW bodies is a consequence of microRNA genesis. EMBO Rep. **7:**904–910.
52. **Raymond, T., E. Gorbunova, I. N. Gavrilovskaya, and E. R. Mackow.** 2005. Pathogenic hantaviruses bind plexin-semaphorin-integrin domains present at the apex of inactive, bent αvβ3 integrin conformers. Proc. Natl. Acad. Sci. U. S. A. **102:**1163–1168.
53. **Reynolds, L. E., L. Wyder, J. C. Lively, D. Taverna, S. D. Robinson, X. Huang, D. Sheppard, R. O. Hynes, and K. M. Hodivala-Dilke.** 2002. Enhanced pathological angiogenesis in mice lacking beta3 integrin or beta3 and beta5 integrins. Nat. Med. **8:**27–34.
54. **Robinson, S. D., L. E. Reynolds, L. Wyder, D. J. Hicklin, and K. M. Hodivala-Dilke.** 2004. Beta3-integrin regulates vascular endothelial growth factor-A-dependent permeability. Arterioscler. Thromb. Vasc. Biol. **24:**2108–2114.
55. **Sand, M., T. Gambichler, D. Sand, M. Skrygan, P. Altmeyer, and F. G. Bechara.** 2009. MicroRNAs and the skin: tiny players in the body's largest organ. J. Dermatol. Sci. **53:**169–175.
56. **Sarnow, P., C. L. Jopling, K. L. Norman, S. Schutz, and K. A. Wehner.** 2006. MicroRNAs: expression, avoidance and subversion by vertebrate viruses. Nat. Rev. Microbiol. **4:**651–659.
57. **Schmaljohn, C., and B. Hjelle.** 1997. Hantaviruses: a global disease problem. Emerg. Infect. Dis. **3:**95–104.
58. **Schmaljohn, C. S.** 2001. Bunyaviridae and their replication, p. 1581–1602. In D. M. Knipe, P. M. Howley, et al. (ed.), Fields virology, 4th ed. Lippincott Williams & Wilkins, Philadelphia, PA.
59. **Sheldon, H., M. Andre, J. A. Legg, P. Heal, J. M. Herbert, R. Sainson, A. S. Sharma, J. K. Kitajewski, V. L. Heath, and R. Bicknell.** 2009. Active involvement of Robo1 and Robo4 in filopodia formation and endothelial cell motility mediated via WASP and other actin nucleation-promoting factors. FASEB J. **23:**513–522.
60. **Somanath, P. R., N. L. Malinin, and T. V. Byzova.** 2009. Cooperation between integrin alphavbeta3 and VEGFR2 in angiogenesis. Angiogenesis **12:**177–185.
61. **Suurna, M. V., S. L. Ashworth, M. Hosford, R. M. Sandoval, S. E. Wean, B. M. Shah, J. R. Bamburg, and B. A. Molitoris.** 2006. Cofilin mediates ATP depletion-induced endothelial cell actin alterations. Am. J. Physiol. Renal Physiol. **290:**F1398–F1407.
62. **Taniguchi, K., R. Kohno, T. Ayada, R. Kato, K. Ichiyama, T. Morisada, Y. Oike, Y. Yonemitsu, Y. Maehara, and A. Yoshimura.** 2007. Spreds are essential for embryonic lymphangiogenesis by regulating vascular endothelial growth factor receptor 3 signaling. Mol. Cell. Biol. **27:**4541–4550.
63. **Tie, J., Y. Pan, L. Zhao, K. Wu, J. Liu, S. Sun, X. Guo, B. Wang, Y. Gang, Y. Zhang, Q. Li, T. Qiao, Q. Zhao, Y. Nie, and D. Fan.** 2010. MiR-218 inhibits invasion and metastasis of gastric cancer by targeting the Robo1 receptor. PLoS Genet. **6:**e1000879.
64. **Toshima, J., J. Y. Toshima, T. Amano, N. Yang, S. Narumiya, and K. Mizuno.** 2001. Cofilin phosphorylation by protein kinase testicular protein kinase 1 and its role in integrin-mediated actin reorganization and focal adhesion formation. Mol. Biol. Cell **12:**1131–1145.
65. **Urbich, C., A. Kuehbacher, and S. Dimmeler.** 2008. Role of microRNAs in vascular diseases, inflammation, and angiogenesis. Cardiovasc. Res. **79:**581–588.
66. **Urbich, C., L. Rossig, D. Kaluza, M. Potente, J. N. Boeckel, A. Knau, F. Diehl, J. G. Geng, W. K. Hofmann, A. M. Zeiher, and S. Dimmeler.** 2009. HDAC5 is a repressor of angiogenesis and determines the angiogenic gene expression pattern of endothelial cells. Blood **113:**5669–5679.
67. **Wang, S., A. B. Aurora, B. A. Johnson, X. Qi, J. McAnally, J. A. Hill, J. A. Richardson, R. Bassel-Duby, and E. N. Olson.** 2008. The endothelial-specific microRNA miR-126 governs vascular integrity and angiogenesis. Dev. Cell **15:**261–271.
68. **Wang, S., and E. N. Olson.** 2009. AngiomiRs—key regulators of angiogenesis. Curr. Opin. Genet. Dev. **19:**205–211.
69. **Winter, J., S. Jung, S. Keller, R. I. Gregory, and S. Diederichs.** 2009. Many roads to maturity: microRNA biogenesis pathways and their regulation. Nat. Cell Biol. **11:**228–234.
70. **Zaki, S., P. Greer, L. Coffield, C. Goldsmith, K. Nolte, K. Foucar, R. Feddersen, R. Zumwalt, G. Miller, P. Rollin, T. Ksiazek, S. Nichol, and C. Peters.** 1995. Hantavirus pulmonary syndrome: pathogenesis of an emerging infectious disease. Am. J. Pathol. **146:**552–579.